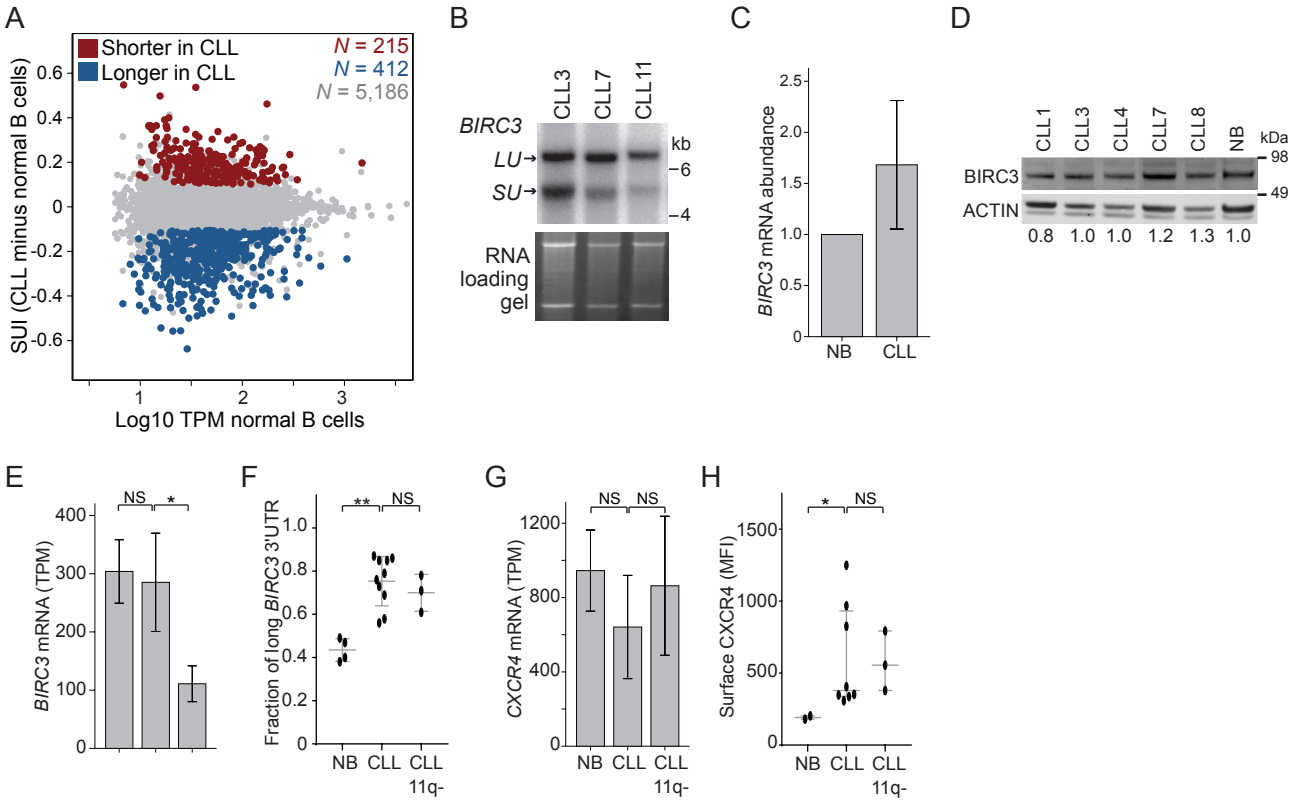
A
Shorter in CLL
Longer in CLL
N = 215
N = 412
N = 5,186
SUI (CLL minus normal B cells)
Log10 TPM normal B cells
B
CLL3
CLL7
CLL11
BIRC3
LU
SU
kb
6
4
RNA loading gel
C
BIRC3 mRNA abundance
NB
CLL
D
CLL1
CLL3
CLL4
CLL7
CLL8
NB
kDa
98
49
BIRC3
ACTIN
0.8 1.0 1.0 1.2 1.3 1.0
E
BIRC3 mRNA (TPM)
NS
*
F
Fraction of long BIRC3 3'UTR
**
NS
NB
CLL
CLL 11q-
G
CXCR4 mRNA (TPM)
NS
NS
H
Surface CXCR4 (MFI)
*
NS

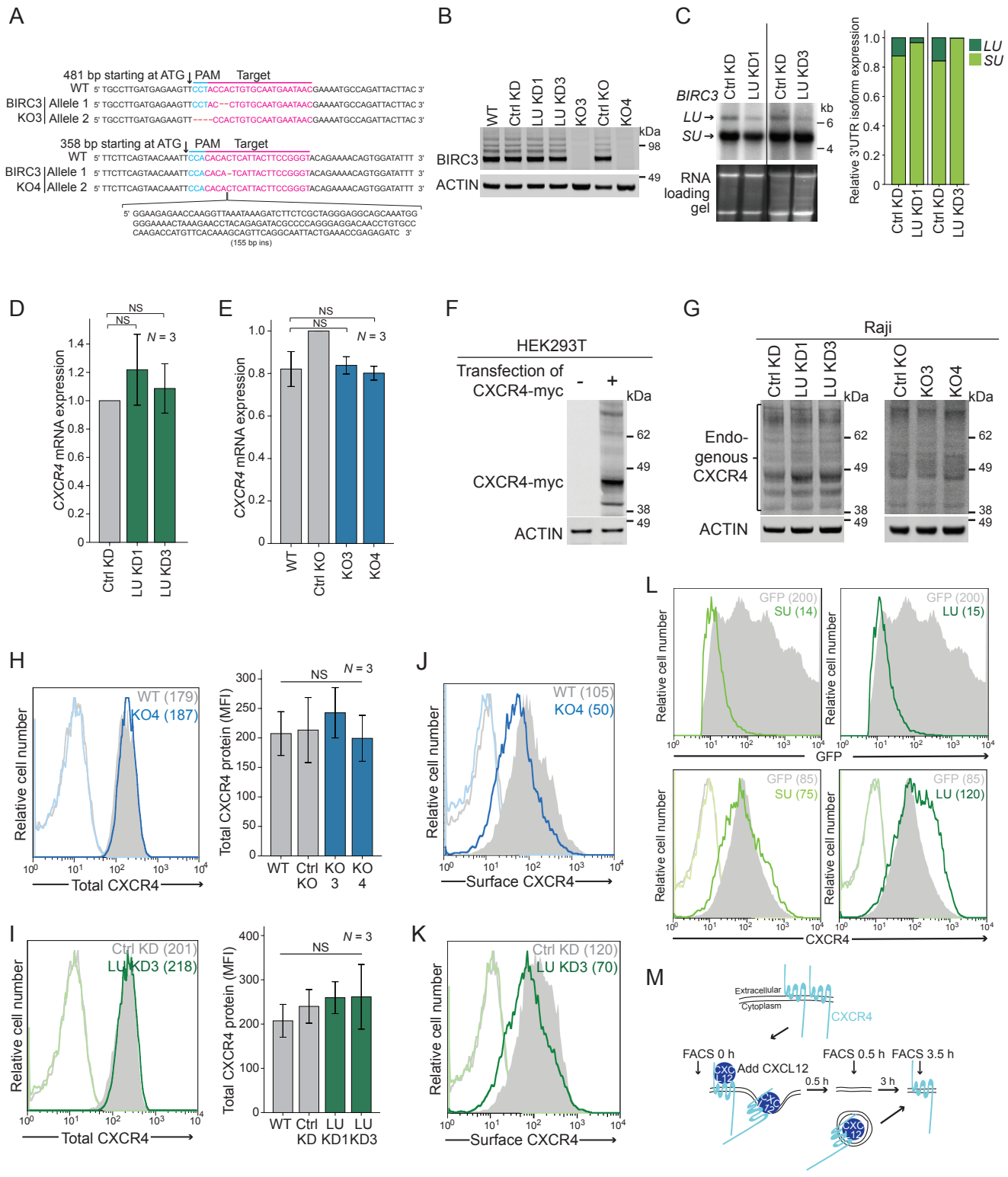
A
481 bp starting at ATG
PAM
Target
WT
BIRC3 | Allele 1
KO3 | Allele 2
358 bp starting at ATG
KO4 | Allele 2
(155 bp ins)
B
WT
Ctrl KD
LU KD1
LU KD3
KO3
Ctrl KO
KO4
kDa
BIRC3
ACTIN
C
BIRC3
LU
SU
RNA loading gel
Relative 3'UTR isoform expression
D
CXCR4 mRNA expression
N = 3
NS
E
F
HEK293T
Transfection of CXCR4-myc
CXCR4-myc
G
Raji
Endo-genous CXCR4
H
WT (179)
KO4 (187)
Relative cell number
Total CXCR4
Total CXCR4 protein (MFI)
I
Ctrl KD (201)
LU KD3 (218)
J
WT (105)
KO4 (50)
Surface CXCR4
K
Ctrl KD (120)
LU KD3 (70)
L
GFP (200)
SU (14)
LU (15)
GFP (85)
SU (75)
LU (120)
GFP
CXCR4
M
Extracellular
Cytoplasm
CXCR4
FACS 0 h
Add CXCL12
FACS 0.5 h
FACS 3.5 h
0.5 h
3 h

A

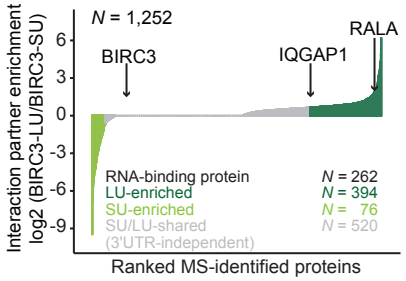

B

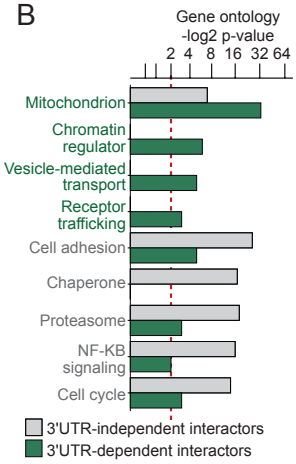

C

Interaction candidate	AA length	Unique peptides	LU/SU ratio
GFP-BIRC3	842	42	1.02
XIAP	497	6	0.87
DIABLO	239	8	1.56
HSPA9	679	25	1.58
TIMM44	452	8	2.56
IQGAP1	1657	27	1.52
RALA	206	5	3.17
SMARCA4	1647	8	1.40
SAMRCA5	1052	39	1.50
ATP5B	529	21	1.50
BAZ1B	1483	16	1.50

D

E

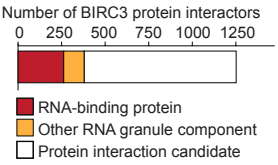

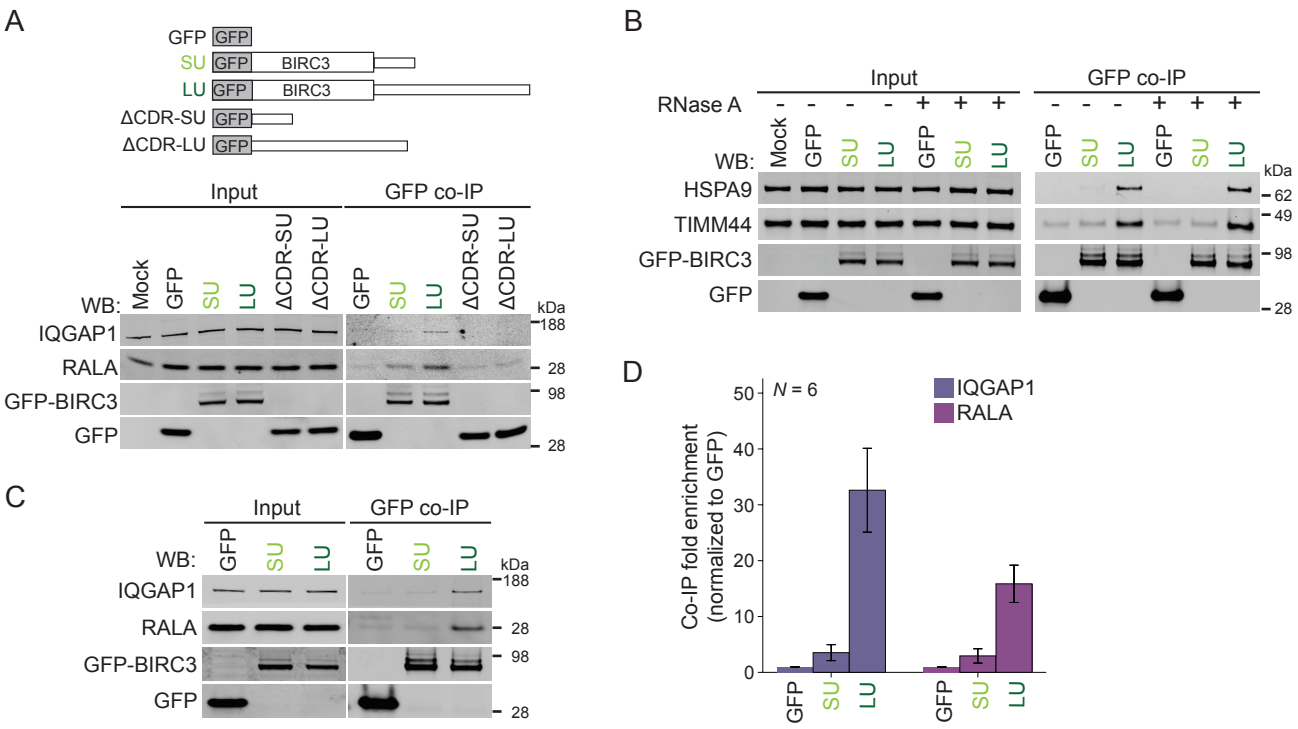
A
GFP
SU
LU
ΔCDR-SU
ΔCDR-LU
BIRC3
Input
GFP co-IP
WB:
Mock
ΔCDR-SU
ΔCDR-LU
IQGAP1
RALA
GFP-BIRC3
kDa
188
28
98
B
RNase A
HSPA9
TIMM44
62
49
C
D
N = 6
Co-IP fold enrichment
(normalized to GFP)
50
40
30
20
10
0

A

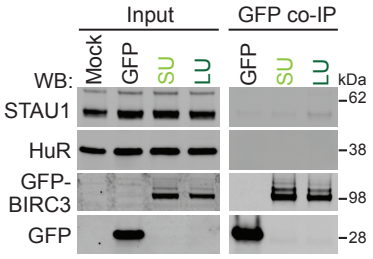

B

RNA-binding protein	AA length	Unique peptides	LU/SU ratio
STAU1	577	3	2.04
HuR	326	9	1.58
IGF2BP1	577	20	1.59
hnRNPA1	327	18	1.46
hnRNPQ	623	16	1.54
CTR9	1173	5	1.0
YBX1	324	8	1.37
SF3B1	1304	29	1.30
FUS	526	8	1.56
KHSRP	711	12	1.32
NUDT21	227	2	0.53
hnRNPC	306	13	1.77
DDX17	729	28	1.31
snRNP70	437	4	1.57

C

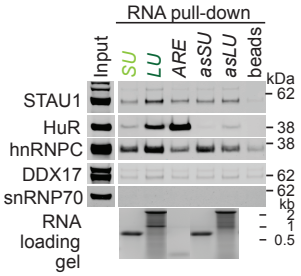

D

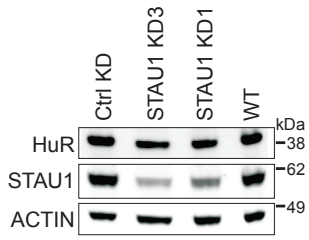

E

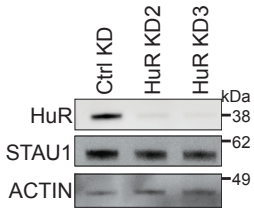

F

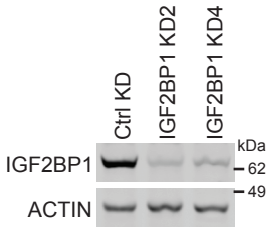

G

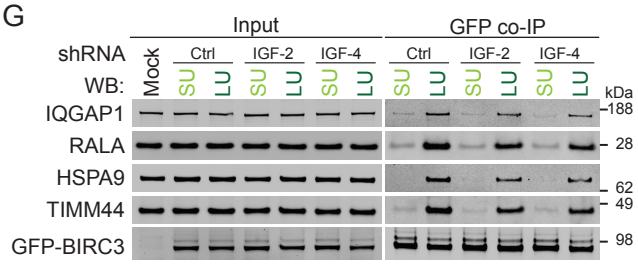

H

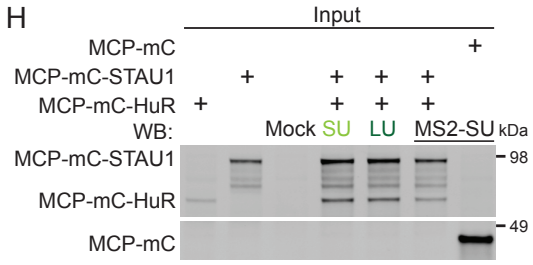

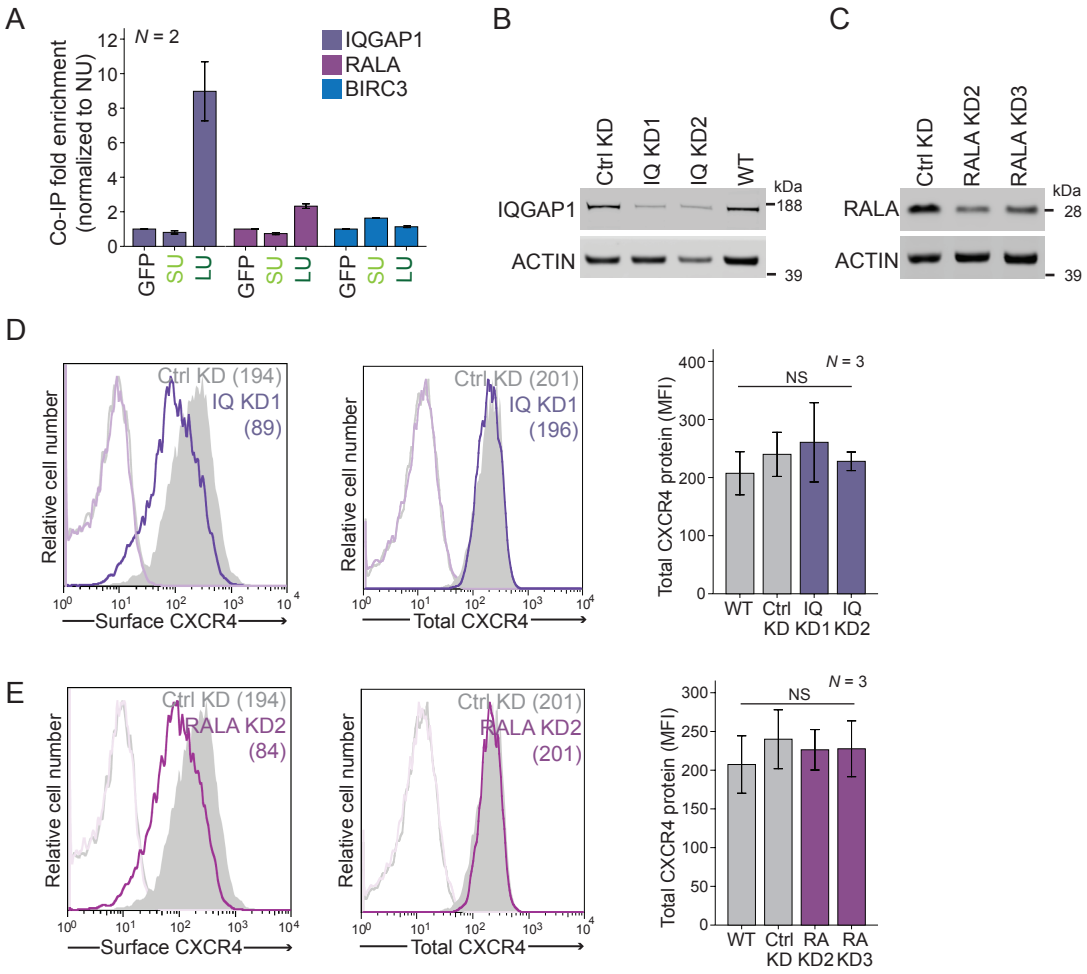
A
N = 2
IQGAP1
RALA
BIRC3
Co-IP fold enrichment (normalized to NU)
GFP
SU
LU
B
Ctrl KD
IQ KD1
IQ KD2
WT
kDa
IQGAP1
188
ACTIN
39
C
Ctrl KD
RALA KD2
RALA KD3
kDa
RALA
28
ACTIN
39
D
Ctrl KD (194)
IQ KD1 (89)
Relative cell number
Surface CXCR4
Ctrl KD (201)
IQ KD1 (196)
Total CXCR4
N = 3
NS
Total CXCR4 protein (MFI)
WT
Ctrl KD
IQ KD1
IQ KD2
E
Ctrl KD (194)
RALA KD2 (84)
Ctrl KD (201)
RALA KD2 (201)
RA KD2
RA KD3

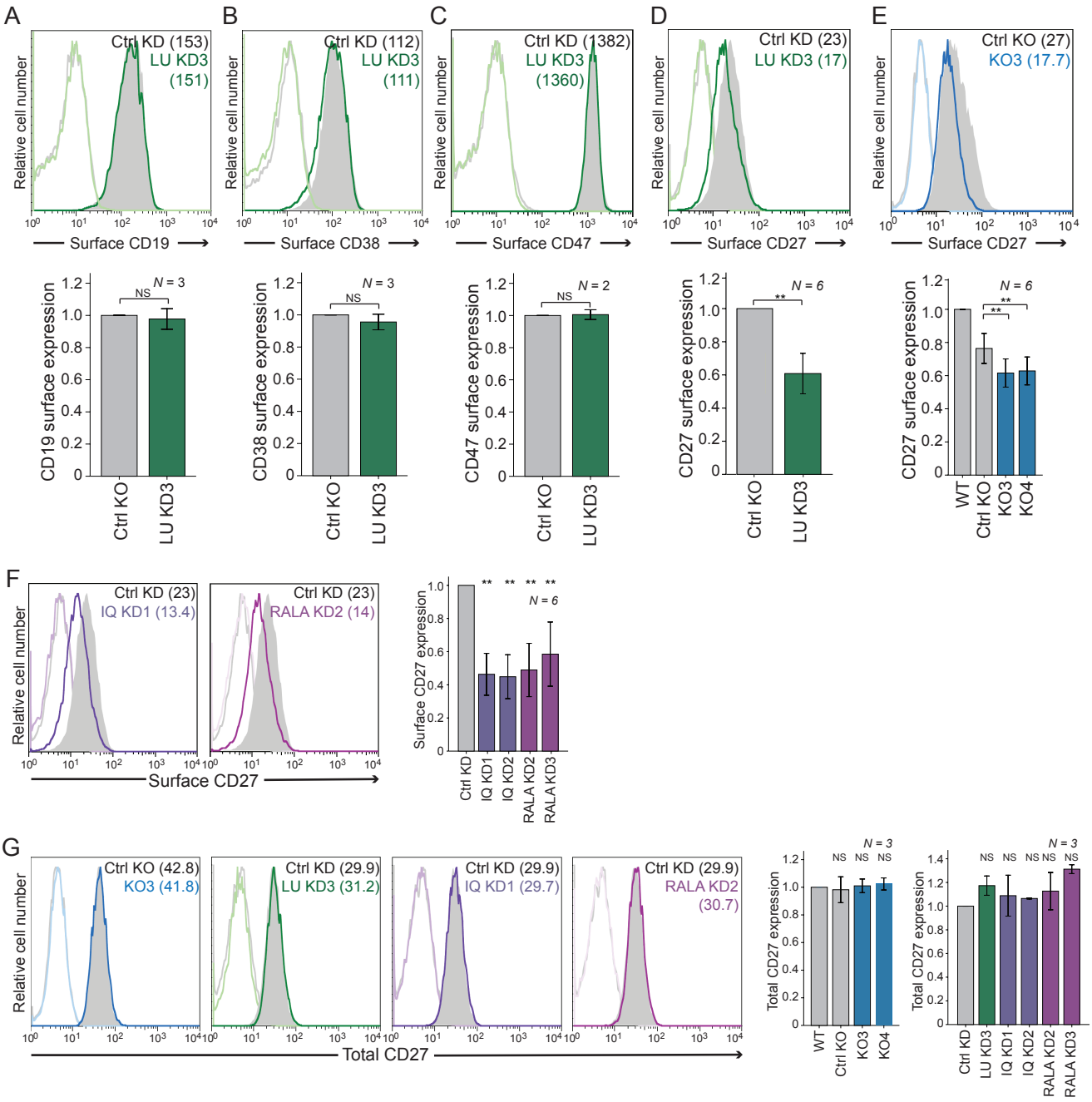
A
Ctrl KD (153)
LU KD3 (151)
Relative cell number
Surface CD19
B
Ctrl KD (112)
LU KD3 (111)
Surface CD38
C
Ctrl KD (1382)
LU KD3 (1360)
Surface CD47
D
Ctrl KD (23)
LU KD3 (17)
Surface CD27
E
Ctrl KO (27)
KO3 (17.7)
Surface CD27
CD19 surface expression
CD38 surface expression
CD47 surface expression
CD27 surface expression
NS
N = 3
N = 2
N = 6
**
Ctrl KO
LU KD3
WT
KO3
KO4
F
Ctrl KD (23)
IQ KD1 (13.4)
Ctrl KD (23)
RALA KD2 (14)
Surface CD27
Surface CD27 expression
Ctrl KD
IQ KD1
IQ KD2
RALA KD2
RALA KD3
G
Ctrl KO (42.8)
KO3 (41.8)
Ctrl KD (29.9)
LU KD3 (31.2)
Ctrl KD (29.9)
IQ KD1 (29.7)
Ctrl KD (29.9)
RALA KD2 (30.7)
Total CD27
Total CD27 expression
N = 3
NS

Supplemental Figure legends

Figure S1. Increased expression of longer 3′UTR isoforms in CLL, Related to Figure 1.

(A) Difference in SUI between CLL and normal CD5+ B cells. SUI is the 'short UTR index'. It is calculated for each gene and is the fraction of 3′-seq reads that map to the most proximal polyadenylation site in the 3′UTR out of all the reads that map to the 3′UTR. All mRNAs that were jointly expressed in normal and malignant B cells with at least two 3′UTR isoforms were plotted. Genes with a statistically significant difference in 3′UTR isoform expression (identified by a generalized linear model using a false disovery rate-adjusted $p < 0.1$ and a usage difference ≥ 0.1) are color-coded and represent the union of shorter or longer 3′UTR isoforms of three CLL samples compared to CD5+ normal B cells ($N = 4$). See also Table S1.

(B) Northern blot showing endogenous *BIRC3* alternative 3′UTR isoform expression of three CLL samples. The RNA gel is shown as loading control.

(C) qRT-PCR validation of *BIRC3* mRNA levels in normal CD5+ B cells ($N = 1$) and CLL B cells ($N = 6$).

(D) Western blot of endogenous BIRC3 protein expression in the samples from Figure 1A. ACTIN was used as loading control.

(E) As in Figure 1C, but showing also CLL samples with 11q deletions ($N = 3$). Mann Whitney test, *, $p = 0.018$.

(F) As in Figure 1B, but showing also CLL samples with 11q deletions ($N = 3$). Mann Whitney test, **, $p = 0.003$.

(G) As in Figure 2H, but showing also CLL samples with 11q deletions ($N = 3$). Mann Whitney test was applied.

(H) As in Figure 2I, but showing also CLL samples with 11q deletions ($N = 3$). Mann Whitney test, *, $p = 0.037$.

Figure S2. BIRC3 regulates surface CXCR4 expression in a 3′UTR-dependent manner, Related to Figure 2.

(A) *BIRC3* genomic locus showing the wild-type sequence and the frame-shift mutations introduced by two different guide RNAs using the CRISPR-Cas9 system.

(B) Western blot of endogenous BIRC3 protein expression in the samples from Figure 2A. ACTIN was used as loading control.

(C) Northern blot showing endogenous *BIRC3* alternative 3′UTR isoform expression of Raji cells stably expressing a ctrl shRNA (ctrl KD) or shRNAs that target the long *BIRC3* 3′UTR isoform (LU KD1, LU KD3). Bands located in lanes located between the depicted samples were

removed. The RNA gel is shown as loading control. The right panel shows quantification of the northern blot.

(D), (E) qRT-PCR of endogenous *CXCR4* mRNA levels in the indicated Raji cell lines. Values were normalized to *HPRT* and show the fold-change relative to ctrl Raji cells (WT, ctrl KD, ctrl KO). Shown is mean ± SD of $N = 3$ biological replicates. Mann Whitney test, p = NS.

(F) Western blot analysis of CXCR4 in HEK293T cells before and after expression of CXCR4-myc. All the visible bands in the right lane reflect CXCR4, as it is highly glycosylated and likely modified by additional post-translational modifications. The predicted size of unmodified CXCR4 is 42 kDa. ACTIN was used as loading control.

(G) Western blot analysis of endogenous CXCR4 in the indicated Raji cell lines. Decreased expression of BIRC3-LU or complete loss of BIRC3 protein does not influence overall CXCR4 protein expression. ACTIN was used as loading control.

(H) FACS analysis of endogenous CXCR4 in Raji cells. The left panel depicts a representative experiment showing fluorescence intensity of total CXCR4 in WT and BIRC3 KO cells. The light grey and and light blue lines represent the isotype controls for the antibody. The grey filled histogram represents the distribution of CXCR4 fluorescence intensities of WT cells and the dark blue line represents the CXCR4 fluorescence intensities of BIRC3 KO cells. The mean fluorescence intensity (MFI) of CXCR4 is shown in parentheses. The right panel shows quantification of total CXCR4 expression in WT, ctrl KO, and BIRC3 KO cells as mean ± SD from ($N = 3$) biological replicates. Mann Whitney test was applied.

(I) As in (H), but showing Raji LU KD cells compared with WT and ctrl KD cells.

(J) Representative experiment showing the fluorescence intensity of surface CXCR4 in WT and BIRC3 KO cells, shown as in Figure S2H (related to Figure 2D).

(K) As in (J), but showing a representative experiment using Raji LU KD cells compared with WT and ctrl KD cells (related to Figure 2E).

(L) Shown are representative FACS plots for the experiment shown in Figure 2F. The top panel shows GFP expression, whereas the bottom panel shows surface CXCR4 expression of the transfected constructs.

(M) Schematic of the CXCR4 recycling assay. CXCR4 surface expression is measured by FACS before and 0.5 h after addition of CXCL12. Ligand binding to CXCR4 results in receptor internalization. After removal of unbound CXCL12, CXCR4 surface expression was measured again after 3 h to assess CXCR4 recycling back to the plasma membrane.

Figure S3. Identification of 3′UTR-independent and 3′UTR-dependent BIRC3 interactors, Related to Figure 3.

(A) Identification of protein interaction partners of GFP-BIRC3-LU and GFP-BIRC3-SU. Shown is the log2-based enrichment ratio of each protein interaction partner from the heavy versus the light fraction obtained by MS. The total number of proteins detected was *N* = 1,252. 262 of them are RNA-binding proteins which are not true BIRC3 protein interactors (see Figure S5A) and were excluded from gene ontology analysis. 3′UTR-independent interactors (grey) have log2-enrichment ratios of LU/SU ≈ 0, whereas the long 3′UTR-dependent interactors (dark green) have a log2-enrichment ratio of LU/SU >0.585.

(B) *p* values of the enrichment scores obtained from gene ontology analysis is shown for the functional gene classes of 3′UTR-independent (grey) and long 3′UTR-dependent (dark green). The red dotted line shows the cut-off for *p* = 0.05. The figure is related to Figure 3C.

(C) LU/SU ratios of the validated BIRC3 interactors shown in Figure 3D. aa, amino acid.

(D) Protein model of BIRC3 showing six protein-interaction domains (three BIR domains, a UBA, CARD, and RING domain).

(E) The protein interaction candidates identified by GFP co-IP of BIRC3 constructs followed by MS revealed a large number of proteins found in proteomic analyses of RNA granules. RNA-binding proteins (red, *N* = 262), additional proteins found in RNA granules (orange, *N* = 118). Taken together, more than 30% of candidate interactors are known components of RNA granules.

Figure S4. The 3′UTR-dependent interaction between IQGAP1, RALA and BIRC3-LU requires newly translated BIRC3, Related to Figure 4.

(A) Co-IP of endogenous IQGAP1 and endogenous RALA using GFP-trap after transfection of the indicated constructs. In addition to GFP, GFP-BIRC3-SU or GFP-BIRC3-LU, also constructs were transfected into HEK293T cells that contain the short or long *BIRC3* 3′UTR, but that lack the BIRC3 coding region (ΔCDR-SU, ΔCDR-LU). 1% of input was loaded.

(B) Co-IP of endogenous HSPA9 and endogenous TIMM44 using GFP-trap after transfection of GFP, GFP-BIRC3-SU or GFP-BIRC3-LU into HEK293T cells. GFP co-IP was performed in the presence or absence of RNase A. 1% of input was loaded.

(C) Co-IP of endogenous IQGAP1 and endogenous RALA using GFP-trap after transfection of GFP, GFP-BIRC3-SU or GFP-BIRC3-LU into HEK293T cells. This figure shows a biological replicate experiment for Figures 3D and 4D.

(D) Quantification of the GFP co-IPs using GFP-BIRC3 constructs. Shown is mean ± SD from *N* = 6 biological replicates. The bands were quantified using ImageJ and were normalized to the values obtained by GFP.

Figure S5. STAU1 and HuR are necessary and sufficient for recruitment of the 3′UTR-dependent protein interaction partners, IQGAP1 and RALA, to BIRC3-LU, Related to Figure 5.

(A) As in Figure 4D, but the RNA-binding proteins HuR and STAU1 were probed by western blot analysis.

(B) List of RNA-binding proteins tested by RNA affinity pull-down for their binding to the alternative *BIRC3* 3′UTRs. This list is related to Figures 5A, 5B, and S5C.

(C) As in Figure 4C, but shown are endogenously expressed RNA-binding proteins in HEK293T cells that were pulled-down using the indicated biotinylated RNAs. *ARE* is a repeated AU-rich element that serves as positive control for HuR. as, antisense fragments. 2% of input was loaded.

(D) Western blot analysis of endogenously expressed STAU1 and HuR protein in HEK293T cells stably expressing a control shRNA (ctrl KD) or stably expressing shRNAs against STAU1 (STAU1 KD1, STAU1 KD3). ACTIN was used as loading control.

(E) As in (D), but western blot was performed in HEK293T cells stably expressing shRNAs against HuR (HuR KD2, HuR KD3).

(F) As in (D), but western blot was performed in HEK293T cells stably expressing shRNAs against IGF2BP1 (IGF2BP1 KD2, IGF2BP1 KD4).

(G) As in Figure 4D, but after stable expression of shRNAs against IGF2BP1 (IGF-2, corresponds to IGF2BP1 KD2, IGF-4 corresponds to IGF2BP1 KD4) or of a control shRNA (ctrl shRNA). In addition to endogenous IQGAP1 and RALA, also the co-IP of endogenous HSPA9 and TIMM44 was interrogated by western blot analysis.

(H) Additional input panels for the co-IP of Figure 5F show the expression levels of MCP-mC-STAU1, MCP-mC-HuR, and MCP-mC alone. 1% of input was loaded.

Figure S6. IQGAP1 and RALA do not regulate total CXCR4 levels, Related to Figure 6.

(A) Quantification of the CXCR4-myc co-IP shown in Figure 6A. Shown is mean ± SD from *N* = 2 biological replicates, normalized to the values obtained by BIRC3-NU.

(B) Western blot analysis of endogenously expressed IQGAP1 protein in WT Raji cells, Raji cells stably expressing a control shRNA (ctrl KD), or stably expressing shRNAs against IQGAP1 (IQ KD1, IQ KD2). ACTIN was used as loading control.
(C) As in (B), but cells stably expressing shRNAs against RALA are shown.
(D) FACS analysis of endogenous CXCR4 in Raji cells. The left panel depicts a representative experiment showing the distribution of fluorescence intensities of surface CXCR4 in ctrl KD and IQ KD Raji cells (related to Figure 6D). The middle panel depicts a representative experiment showing the distribution of fluorescence intensities of total CXCR4 in ctrl KD and IQ KD cells, shown as in Figure S2H. The right panel shows quantification of total CXCR4 expression in WT, ctrl KD and IQ KD Raji cells as mean ± SD from (N = 3) biological replicates. Mann Whitney test was applied.
(E) As in (D), but cells with stable KD of RALA (RA KD2, RA KD3) are shown. The left panel is related to Figure 6E.

Figure S7. BIRC3-LU, IQGAP1, and RALA regulate surface expression of CD27 receptor, Related to Figure 2.
(A-D) FACS analysis of surface levels of endogenously expressed receptors in Raji cells stably expressing the indicated shRNAs. Representative experiments are shown in the top panels as in Figure S2H. The bottom panels show the mean ± SD from biological replicates. Mann Whitney test was applied. **, p = 0.003.
(E) As in (D), but comparing surface CD27 levels in ctrl KO versus BIRC3 KO cells.
(F) As in (D), but comparing surface CD27 levels in ctrl KD versus Raji cells expressing shRNAs against IQGAP1 (IQ KD) or RALA. Mann Whitney test was applied **, P = 0.003.
(G) As in (D), but comparing the effects of the indicated knock-downs or knock-outs on total CD27 expression.